Separating Reflective and Fluorescent Components Using High Frequency Illumination in the Spectral Domain

Ying Fu[1], Antony Lam[2], Imari Sato[2], Takahiro Okabe[3], Yoichi Sato[1]
[1]The University of Tokyo [2]National Institute of Informatics [3]Kyushu Institute of Technology

Abstract

Hyperspectral imaging is beneficial to many applications but current methods do not consider fluorescent effects which are present in everyday items ranging from paper, to clothing, to even our food. Furthermore, everyday fluorescent items exhibit a mix of reflectance and fluorescence. So proper separation of these components is necessary for analyzing them. In this paper, we demonstrate efficient separation and recovery of reflective and fluorescent emission spectra through the use of high frequency illumination in the spectral domain. With the obtained fluorescent emission spectra from our high frequency illuminants, we then present to our knowledge, the first method for estimating the fluorescent absorption spectrum of a material given its emission spectrum. Conventional bispectral measurement of absorption and emission spectra needs to examine all combinations of incident and observed light wavelengths. In contrast, our method requires only two hyperspectral images. The effectiveness of our proposed methods are then evaluated through a combination of simulation and real experiments. We also demonstrate an application of our method to synthetic relighting of real scenes.

1. Introduction

Hyperspectral reflectance data are beneficial to many applications including but not limited to archiving for cultural e-heritage [1], medical imaging [2], and also color relighting of scenes [3]. As a result, many methods for acquiring the spectral reflectance of scenes have been proposed [4, 5, 6, 7, 8, 9]. Despite the success of these methods, they have all made the assumption that fluorescence is absent from the scene. However, fluorescence does frequently occur in many objects. In fact, Barnard shows that fluorescent surfaces are present in 20% of randomly constructed scenes [10]. This is a significant proportion of scenes that have not been considered by past methods.

Another important point is that reflective and fluorescent components behave very differently under different illuminants [3, 11]. Thus to accurately predict the color of objects, separate modeling of all spectral properties of both reflective and fluorescent components is essential. Specifically, when a reflective surface is illuminated by incident light, it reflects back light of the same wavelength. Fluorescent surfaces on the other hand, first absorb incident light and then emit at longer wavelengths. This wavelength shifting property is known as Stokes shift [12, 13] and the question of which wavelengths of light are absorbed and which wavelengths are emitted are defined by the fluorescent surface's absorption and emission spectrum (Figure 2).

(a) White light (b) Reflection (c) Fluorescence

Figure 1. (a) The scene captured under white light. (b) The recovered reflective component. (c) The recovered fluorescent component.

The goal of this paper is to accurately recover the full spectral reflective and fluorescent components of an entire scene. Typical fluorescent objects exhibit both reflectance and fluorescence (Figure 1(a)). So the question of how these components can be accurately separated also needs to be addressed. In this paper, we show that the reflective and fluorescent spectra of a scene can be efficiently separated and measured through the use of high frequency illumination in the spectral domain. Our approach only assumes that the absorption spectrum of the fluorescent material is a smooth function with respect to the frequency of the lighting in the spectral domain. With this assumption, it becomes possible to separate reflective and fluorescent components by just two hyperspectral images taken under a high frequency illumination pattern and its shifted version in the spectral domain. We show that the reflective and fluorescent emission spectra can then be fully recovered by our separation method.

What is interesting is that an analogy can be drawn between our approach and that of Nayar *et al.* [14]. Nayar *et al.* devised a way to separate direct and indirect components using high frequency lighting patterns in the spatial

1550-5499/13 $31.00 © 2013 IEEE
DOI 10.1109/ICCV.2013.63

domain. We find that reflectance and fluorescence in the spectral domain can be thought of as similar to direct and indirect illumination in the spatial domain. More specifically, the reflective component may be thought of as a direct component in the spectral domain because incident light is reflected back at the same wavelength. The fluorescent component on the other hand, does not emit light at the same wavelength as incident light. This is because it always shifts incident light from shorter wavelengths to longer ones. So one can think of it as indirect lighting in the spectral domain.

In addition to recovering reflectance and fluorescent emission spectra, we also make the observation that materials with similar emission spectra tend to have similar absorption spectra as well. Using this observation, we devise a method for taking the recovered emission spectra from high frequency lighting and estimate their corresponding absorption spectra. There are well established methods for measuring fluorescent spectra [15]. For example, bispectral methods are effective approaches that measure fluorescence in terms of incoming and outgoing wavelengths but only work for a single point in space. Thus making the capture of entire scenes very labor and time intensive.

In summary, our contributions are that we devise a method for efficient separation and recovery of full reflectance and fluorescent emission spectra and we present, to our knowledge, the first method for estimating the absorption spectrum of a material given its emission. Since we completely recover the reflective and fluorescent emission and absorption spectra of the scene, we also show our ability to accurately predict the relighting of scenes under novel lighting.

2. Related Work

As noted earlier, there have been a number of papers on recovering the spectral reflectance of scenes [4, 5, 6, 7, 8, 9]. Despite the effectiveness of these methods for spectral reflectance capture, they all do not take the effects of fluorescence into account.

Unfortunately, not accounting for fluorescence can have a detrimental affect on color accuracy. For example, Johnson and Fairchild [3] showed that considering fluorescence can dramatically improve color renderings. Hullin *et al.* [16] showed the importance of modeling and rendering of reflective-fluorescent materials using their bidirectional reflectance and reradiation distribution functions (BRRDF). Besides color rendering, the observation of fluorescent emissions on an object's surface has also been applied to photometric stereo for shape reconstruction [17, 18]. As mentioned earlier, Barnard *et al.* concluded that fluorescent surfaces are present in 20% of randomly constructed scenes [10]. Thus the presence of fluorescence is significant and warrants attention.

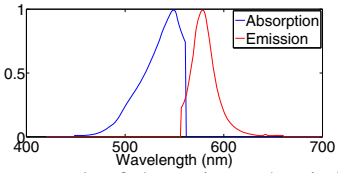

Figure 2. An example of absorption and emission spectra.

In practice, fluorescent objects typically exhibit both reflectance and fluorescence so the joint occurrence of these phenomenon in scenes needs to be considered. Some methods in the literature have given this issue attention. Alterman *et al.* [19] separated the appearance of fluorescent dyes from a mixture by unmixing multiplexed images. Zhang and Sato [11] derived an independent component analysis based method to estimate the RGB colors of reflectance and fluorescent emission but not their spectral distributions. They also did not estimate the excitation spectra of the fluorescent component and so, cannot predict intensity changes in fluorescent emission due to different illumination spectra. Lee *et al.* [20] provided a mathematical description for fluorescent processes and recovered the additive spectra of reflective and fluorescent components but did not separate them. Tominaga *et al.* [21] estimated fluorescent emission spectra using multispectral images taken under two ordinary light sources. A limitation is that they assumed fluorescent emissions to be constant for all absorption wavelengths and thus cannot accurately predict the brightness of fluorescent components under varying illumination. Finally, none of these methods fully recover all reflective and fluorescent spectral components of scenes.

As mentioned earlier, one of the key challenges in our problem is the separation of reflective and fluorescent components from composite objects exhibiting both phenomenon. There have been a number of methods in the literature on separating components in images. For example, Farid and Adelson [22] used independent components analysis to separate reflections on glass and a painting on the side of the glass opposite the observer. Nayar *et al.* [23] separated specular reflections from diffuse reflections. As mentioned earlier, there is an analogy between our spectral domain work and the spatial domain work of Nayar *et al.* [14]. In this work, we show the effectiveness of using high frequency lighting in the spectral domain, not the spatial domain, for our separation and spectral recovery problem.

3. Separation of Reflection and Fluorescence

3.1. Reflection and Fluorescence Models

We begin with a brief review of how reflective-fluorescent materials are modeled [11]. Since reflection and fluorescence have different physical behaviors, they need to be described by different models.

The radiance of a reflective surface depends on incident light and its reflectance. The observed radiance of an ordi-

nary reflective surface at wavelength λ is computed as

$$p_r(\lambda) = l(\lambda)r(\lambda) \tag{1}$$

where $l(\lambda)$ is the spectrum of the incident light at wavelength λ and $r(\lambda)$ is the spectral reflectance of the surface at wavelength λ.

The observed radiance of a pure fluorescent surface depends on the incident light, the material's absorption spectrum, and its emission spectrum. Fluorescence typically absorbs light at some wavelengths and emits them at longer wavelengths. The way this works is that when incident light hits a fluorescent surface, the surface's absorption spectrum will determine how much of the light is absorbed. Some of the absorbed energy is then released in the form of an emission spectrum at longer wavelengths than the incident light. The remainder of the absorbed energy is released as heat. Figure 2 illustrates an example of the absorption and emission spectra for a fluorescent material over the visible spectrum.

Let $l(\lambda')$ represent the intensity of the incident light at wavelength λ', the observed spectrum of a pure fluorescent surface [11] at wavelength λ is described in terms of its absorption and emission spectra as

$$p_f(\lambda) = \left(\int l(\lambda^{'})a(\lambda^{'})\mathrm{d}\lambda^{'} \right) e(\lambda) \tag{2}$$

where $a(\lambda^{'})$ and $e(\lambda)$ represent the absorption and emission spectrum. Equation (2) [1]can be rewritten with $k = \left(\int l(\lambda^{'})a(\lambda^{'})\mathrm{d}\lambda^{'} \right)$ as $p_f(\lambda) = ke(\lambda)$, which means that the shape or the distribution of the emitted spectrum is constant, but the scale k of the emitted spectrum changes under different illuminations. Namely, the radiance of the fluorescent emission changes under different illuminations, but its color stays the same regardless of illumination color.

From Equations (1) and (2), the radiance of a reflective-fluorescent surface point is

$$p(\lambda) = l(\lambda)r(\lambda) + \left(\int l(\lambda^{'})a(\lambda^{'})\mathrm{d}\lambda^{'} \right) e(\lambda). \tag{3}$$

3.2. Separation Using High Frequency Illumination

In our experiments, we use high frequency illumination defined in the spectral domain for separating reflective and fluorescent components. Let us start with simple binary illuminants to describe the key idea of our method. We denote a high-frequency illumination pattern shown in Figure 3(b) by $l_1(\lambda)$ and its complement shown in Figure 3(c) by $l_2(\lambda)$. The illuminants are defined such that when $l_1(\lambda)$ has intensity, $l_2(\lambda)$ has no intensity and vice versa. Let us consider a certain wavelength λ_1 where $l_1(\lambda_1) = 1$ and $l_2(\lambda_1) = 0$.

[1]This model assumes that there is little overlap between the absorption and emission spectra. As far as we examined fluorescent materials in the McNamara and Boswell fluorescent spectral dataset, such overlap tends to be small, and therefore the model can approximate the real model well.

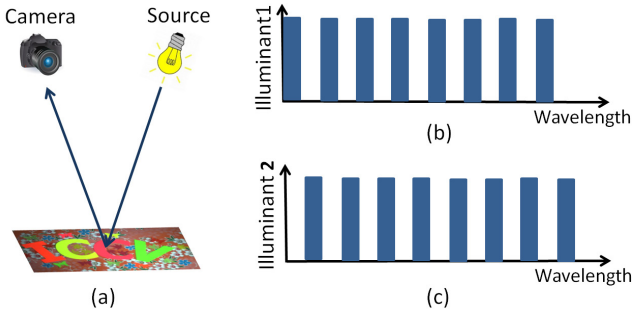

Figure 3. An example of a captured scene (a). When a reflective-fluorescent point in the scene is lit by the illuminant (b), which is a high frequency binary illumination pattern in the wavelength domain, each lit wavelength includes both reflective and fluorescent components while the unlit wavelengths have only the fluorescent component. (c) shows its complement.

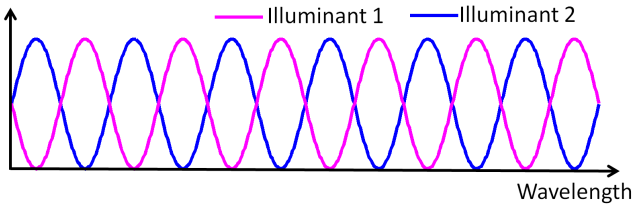

Figure 4. Sinusoidal illuminant patterns. The blue and pink solid lines denote two illumination patterns. There is a phase shift between them.

Since reflection preserves wavelength, we obtain

$$\begin{aligned} p_1(\lambda_1) &= r(\lambda_1) + \frac{1}{2}k'e(\lambda_1), \\ p_2(\lambda_1) &= \frac{1}{2}k'e(\lambda_1). \end{aligned} \tag{4}$$

Here, we assume that $\int l_1(\lambda')a(\lambda')\mathrm{d}\lambda' = \int l_2(\lambda')a(\lambda')\mathrm{d}\lambda' = \int a(\lambda')\mathrm{d}\lambda'/2 = k'/2$. That is, the absorptions due to our high-frequency illumination patterns are the same. We will show later in this section this is true when the absorption $a(\lambda')$ is smooth with respect to the frequency of the illumination patterns in the spectral domain as is similarly discussed for the spatial domain by Nayar *et al.*[14]. With the same absorptions under the two illuminants, we obtain the reflectance and emission spectra at λ_1 as

$$\begin{aligned} r(\lambda_1) &= p_1(\lambda_1) - p_2(\lambda_1), \\ k'e(\lambda_1) &= 2p_2(\lambda_1). \end{aligned} \tag{5}$$

We obtain the reflectance and emission spectra at λ_2 where $l_1(\lambda_2) = 0$ and $l_2(\lambda_2) = 1$ in a similar manner.

In our work, we use high frequency sinusoidal illuminants (Figure 4) in the spectral domain to achieve the same effect as the binary lighting patterns because they are both more practical and fit into the theory of our framework. The illuminants can be represented as $l_1(\lambda) = \alpha + \beta\cos(2\pi f_l\lambda)$ and $l_2(\lambda) = \alpha + \beta\cos(2\pi f_l\lambda + \phi)$, where f_l is the frequency of illumination. The radiance of a surface under

these two sinusoidal illuminants can be described as,

$$\begin{aligned} p_1(\lambda) &= l_1(\lambda)r(\lambda) + k_1 e(\lambda), \\ p_2(\lambda) &= l_2(\lambda)r(\lambda) + k_2 e(\lambda), \\ k_n &= \int l_n(\lambda^{'})a(\lambda^{'})\mathrm{d}\lambda^{'}. \end{aligned} \tag{6}$$

Here, assuming that k_n are constant for l_1 and l_2, that is to say, $k_1 = k_2 = k$, the reflectance $r(\lambda)$ and fluorescent emission $ke(\lambda)$ can be recovered as

$$\begin{aligned} r(\lambda) &= \frac{p_1(\lambda) - p_2(\lambda)}{l_1(\lambda) - l_2(\lambda)}, \\ ke(\lambda) &= p_1(\lambda) - \frac{p_1(\lambda) - p_2(\lambda)}{l_1(\lambda) - l_2(\lambda)} l_1(\lambda). \end{aligned} \tag{7}$$

We now discuss how to satisfy the condition $k_1 = k_2 = k$. In the following, we consider the requirements for our illuminants based on the Nyquist sampling theorem [24] and on an analysis of the McNamara and Boswell fluorescence spectral dataset [25].

The spectrum of sinusoidal illumination $l_1(\lambda)$ in the frequency domain [24] then becomes

$$L_1(f) = \frac{1}{2}[\beta\delta(f - f_l) + 2\alpha\delta(f) + \beta\delta(f + f_l)] \tag{8}$$

where $\delta(f)$ is the Dirac delta function. Let $a_n(\lambda) = l_n(\lambda)a(\lambda)$ $\{n = 1, 2\}$. Let $A(f)$ and $A_n(f)$ denote the Fourier transform of $a(\lambda)$and $a_n(\lambda)$, respectively. Since the product $l_n(\lambda)a(\lambda)$ in the spectral domain corresponds to a convolution in its Fourier domain, the Fourier transform of $a_1(\lambda)$ is

$$A_1(f) = \frac{1}{2}[\beta A(f - f_l) + 2\alpha A(f) + \beta A(f + f_l)] \tag{9}$$

That is, a replication of the Fourier transform of the original signal $A(f)$ is centered around $+f_l$ and 0 and $-f_l$.

The Fourier transform of $l_1(\lambda)$ and $l_2(\lambda)$ with the phase offset ϕ are related as $L_2(f) = e^{i\phi}L_1(f)$, and thus the frequency spectrum of $a_2(\lambda)$ is

$$\begin{aligned} A_2(f) = \frac{1}{2}[&\beta e^{i\phi}A(f - f_l) + 2\alpha A(f) \\ &+ \beta e^{-i\phi}A(f + f_l)] \end{aligned} \tag{10}$$

From the definition of the Fourier transform $A_n(f) = \int_{-\infty}^{+\infty} a_n(\lambda)e^{-i2\pi f\lambda}\mathrm{d}\lambda$, substituting $f = 0$ into this definition, we obtain $A_n(0) = \int_{-\infty}^{+\infty} a_n(\lambda)\mathrm{d}\lambda = \int_{-\infty}^{+\infty} l_n(\lambda)a(\lambda)\mathrm{d}\lambda = k_n$. Therefore, k_n corresponds to $A_n(f)$'s zero-frequency component. This tells us that we need to satisfy the condition $A_1(0) = A_2(0)$ so that $k_1 = k_2 = k$. In Equations (9) and (10), substituting $f = 0$, we obtain $A_1(0) = \frac{1}{2}[\beta A(-f_l) + 2\alpha A(0) + \beta A(f_l)]$ and $A_2(0) = \frac{1}{2}[\beta e^{i\phi}A(-f_l) + 2\alpha A(0) + \beta e^{-i\phi}A(f_l)]$. Let us define f_a as $a(\lambda)$'s maximum frequency. Then $A(-f_l)$ and $A(f_l)$ become zero for $f_l > f_a$. This means that we obtain $A_1(0) = A_2(0) = 2\alpha A(0)$ for $f_l > f_a$ to achieve $k_1 = k_2 = k$. Thus, the frequency of the illuminants in the wavelength domain f_l needs to be greater than $a(\lambda)$'s maximum frequency or bandwidth f_a.

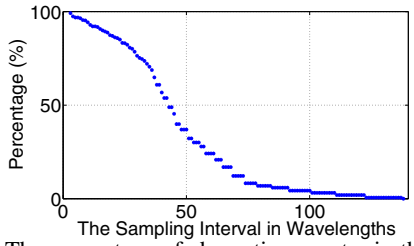

Figure 5. The percentage of absorption spectra in the McNamara and Boswell fluorescence spectral dataset where $k_1 = k_2$ given different sampling intervals. The smaller the sampling interval, the more absorption spectra satisfy our requirement that $k_1 = k_2$.

We now discuss the maximum frequency of $a(\lambda)$ on the McNamara and Boswell fluorescence spectral dataset. We examine the maximum frequency of all 509 materials in the dataset, and obtain the maximum frequency of each absorption spectrum while retaining 99% of the energy[1]. The mean of the maximum frequency for all absorption spectra in the dataset is $1/45.9[nm^{-1}]$ and its standard deviation is $1/24.1[nm^{-1}]$. As mentioned previously, the illumination frequency f_l needs to be greater than $a(\lambda)$'s maximum frequency f_a, and the period is the reciprocal of the frequency, so the period of the illumination – which we call "sampling interval" – in the spectral domain needs to be less than the minimum sampling interval of all absorption spectra of fluorescent materials in the scene. Figure 5 shows the percentage of absorption spectra in the McNamara and Boswell fluorescence spectral dataset that satisfy the condition $k_1 = k_2$ under different sampling intervals. We set the period of the illumination as $40nm$ in our experiments due to limitations of our light source. However, this is still less than the mean minimum sampling interval of all absorption spectra $(45.9nm)$ found in the dataset and works well in practice.

4. Estimating the Absorption Spectra

In this section, we will explain how we estimate the absorption spectrum of a material from its emission spectrum that was obtained using our method in Section 3.2.

The basic observation behind our method is that fluorescent materials with similar emission spectra tend to have similar absorption spectra. From this observation, we derive a method that uses a dictionary of known emission and absorption spectrum pairs to estimate an absorption spectrum from a given novel emission.

Specifically, let $\hat{\boldsymbol{e}}$ be an emission spectrum whose absorption spectrum $\hat{\boldsymbol{a}}$ is unknown. Let $\{\boldsymbol{e}_j\}$ be a dictionary of emission spectra and $\{\boldsymbol{a}_j\}$ be the known corresponding absorption spectra. Representing all these spectra as vectors, we first determine the linear combination of $\{\boldsymbol{e}_j\}$ to

[1]Since there exists some noise in the original spectra, ignoring some high frequency components is reasonable.

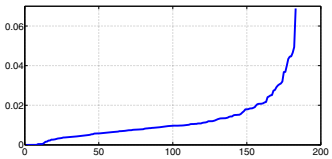

Figure 6. All test errors sorted in ascending order. 67% of cases were below the average error of 0.012.

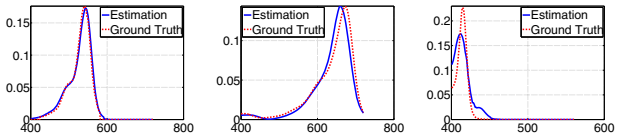

0.005 0.012 0.019

Figure 7. Examples of estimated absorption spectra and their root-mean-square-errors.

reconstruct $\hat{\boldsymbol{e}}$ by solving

$$\hat{\boldsymbol{e}} = \sum_j w_j \boldsymbol{e}_j \tag{11}$$

The weights $\{w_j\}$ are then used to calculate the corresponding excitation spectrum $\hat{\boldsymbol{a}}$ by

$$\hat{\boldsymbol{a}} = \sum_j w_j \boldsymbol{a}_j \tag{12}$$

Let $\{\boldsymbol{e}_j^{'}\}$ and $\{\boldsymbol{a}_j^{'}\}$ denote the subsets of $\{\boldsymbol{e}_j\}$ and $\{\boldsymbol{a}_j\}$ whose corresponding weights $\{w_j \neq 0\}$. Note that using the same $\{w_j\}$ in Equation (11) and (12) requires the linear combination be kept between the subspaces spanned by $\{\boldsymbol{e}_j^{'}\}$ and $\{\boldsymbol{a}_j^{'}\}$. We assert that an emission spectrum can typically be well-represented by a sparse basis. To show this, we perform leave-one-out cross-validation where for each emission spectrum in the McNamara and Boswell fluorescence spectral dataset, we set $\hat{\boldsymbol{e}}$ as the testing sample and use the remaining emission spectra in $\{\boldsymbol{e}_j\}$ as the dictionary. We find that any given emission $\hat{\boldsymbol{e}}$ can on average be well represented by 10 emission spectra from the dictionary, which is very sparse compared to the size of the whole dictionary, Thus $\hat{\boldsymbol{e}}$ can considered to live in a low-dimensional sub-space spanned by $\{\boldsymbol{e}_j^{'}\}$. Therefore, to minimize the number of basis vectors used from $\{\boldsymbol{e}_j\}$, we seek to reconstruct $\hat{\boldsymbol{e}}$ by sparse weights $\boldsymbol{w}$ through l_1-norm minimization [26, 27, 28], according to

$$\min \|\boldsymbol{w}\|_1 \quad s.t. \quad w_j \geq 0 \text{ and } \left\| \hat{\boldsymbol{e}} - \sum_j w_j \boldsymbol{e}_j \right\|_2^2 \leq \epsilon \tag{13}$$

To test the accuracy of our method, we chose a subset of materials from the McNamara and Boswell fluorescence spectral dataset where both the emission and absorption spectra were present in the visible range (400 - 720 nm). This resulted in a collection of 183 materials. We then performed leave-one-out cross-validation using our method and the 183 emission and absorption spectra. The estimated absorption spectrum was then compared against the ground truth using the root-mean-square-error (RMSE).

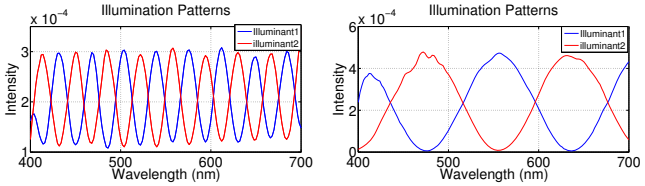

(a) High frequency illuminants produced by ELS

(b) Low frequency illuminants produced by ELS

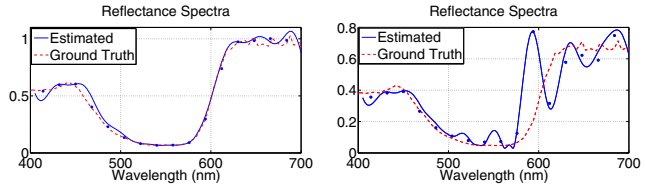

(c) Recovered $r(\lambda)$ under high frequency illuminants

(d) Recovered $r(\lambda)$ under low frequency illuminants

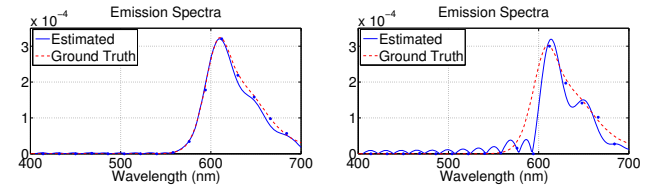

(e) Recovered $e(\lambda)$ under high frequency illuminants

(f) Recovered $e(\lambda)$ under low frequency illuminants

Figure 8. Evaluate the separation method on pink sheet captured.

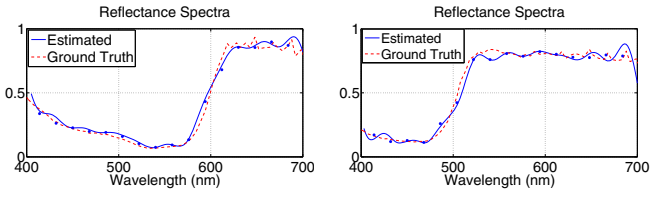

(a) Recovered $r(\lambda)$

(b) Recovered $r(\lambda)$

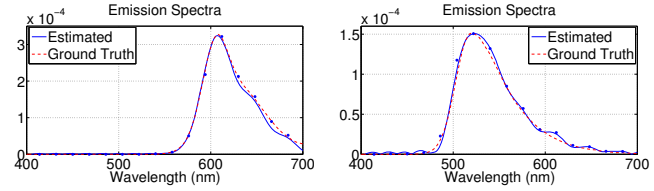

(c) Recovered $e(\lambda)$

(d) Recovered $e(\lambda)$

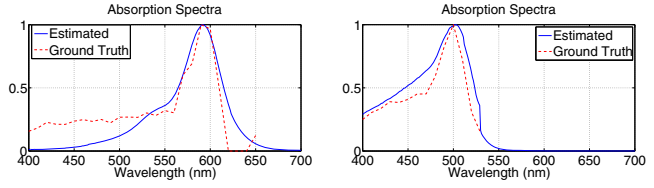

(e) Recovered $a(\lambda)$

(f) Recovered $a(\lambda)$

Figure 9. Recovered reflectance $r(\lambda)$, fluorescent emission $e(\lambda)$ and absorption $a(\lambda)$ spectra of the red and yellow sheets.

The ground truth and estimation were also normalized for scale by setting them to be unit length vectors.

In our results, we obtained an average error of 0.012. See Figure 6 for a plot of all the errors for the 183 estimated absorption spectra. We did find a minority of cases

with high errors that violated our assumption that similar emission spectra map to the same absorption spectra. Despite this, the majority of materials fit our assumption and absorption is accurately estimated as can be seen in Figure 7. We also note that absorption only determines the scale of the emission and not the color of the material. Thus some minor loss in accuracy for estimated absorption does not have a dramatic effect on the predicted color of scenes.

5. Experimental results

In our experiments, we first demonstrate the importance of high frequency illumination using quantitative results on the recovery of reflectance and fluorescent spectra from real scenes. We then present visual examples of separated reflective and fluorescent components as RGB images. In addition, we use our recovered spectra to accurately relight fluorescent scenes.

5.1. Experimental Setup

With the exception of our near UV light, for all other illuminants in our experiments, we use a Nikon Equalized Light Source (ELS). The ELS is a programmable light source that can produce light with arbitrary spectral patterns from 400 nm to 720 nm. We use a PR-670 SpectraScan Spectroradiometer to collect ground truth spectra. For our proposed method, we use a hyperspectral camera (EBA Japan NH-7) to capture whole scenes.

Figure 8(a) shows two high frequency illuminants produced by the ELS. Under these illuminants, we use the hyperspectral camera to capture the scene at wavelengths where either one of these illuminants have peaks so that the difference between l_1 and l_2 would be large and allow for reliable separation.

5.2. Quantitative Evaluation

In this section, we first compare quantitative results on recovering the reflective and fluorescent spectral components using high and low frequency light on fluorescent colored sheets. Figure 8(a) and (b) show spectral distributions of the high frequency and low frequency illuminants used in our experiments.

In Figure 8(c)-(f) we see the recovered reflectance and fluorescent emission spectra of a pink fluorescent sheet under different illuminants. The recovered reflectance (Figure 8(c)) and fluorescent emission spectra (Figure 8(e)) under the high frequency illuminants approximate ground truth well. When the object is captured under the low frequency illuminants, the recovered reflectance (Figure 8(d)) and fluorescent emission (Figure 8(f)) have obvious errors. Figure 9(a)-(d) shows the recovered reflectance and fluorescent emission spectra of red and yellow fluorescent sheets under the high frequency illuminants. All these results demonstrate that our method is able to recover reflectance and fluorescent emission spectra efficiently under high frequency illuminants.

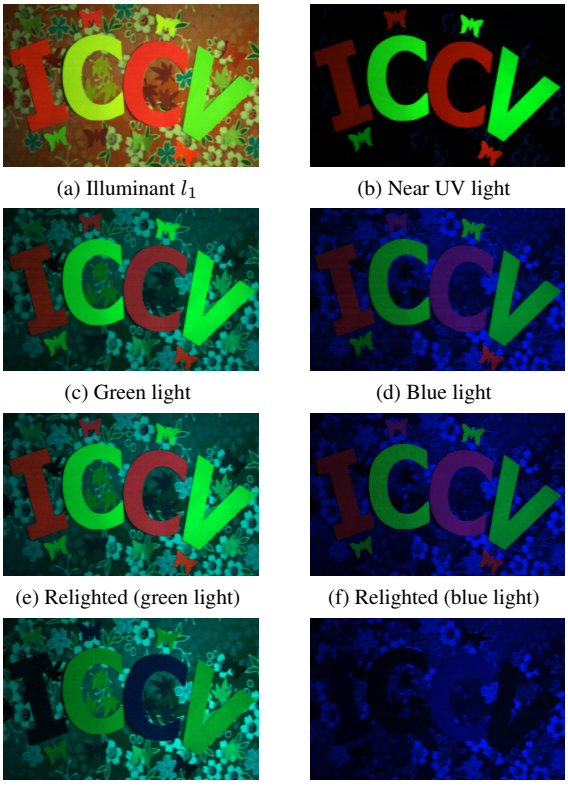

(a) Illuminant l_1 (b) Near UV light (c) Green light (d) Blue light (e) Relighted (green light) (f) Relighted (blue light) (g) Relighted (reflectance only) (h) Relighted (reflectance only)

Figure 10. The relighting results for a scene.

In Figure 9(e) and (f), the recovered fluorescent absorption spectra of the red and yellow fluorescent sheets are shown. Due to limitations of our capture equipment, the ground truth could not be accurately measured in the short wavelength region in cases where absorption was relatively weak. This issue can be seen in the the shorter wavelengths for the red sheet (Figure 9(e)). However, we can see that the recovered absorption spectra and the ground truth measurements still agree quite well.

5.3. Visual Separation and Relighting Results

In this section, we show results for the separation of reflectance and fluorescence as well as accurate relighting performance. Our original results are in the form of hyperspectral images but to easily visualize them, we have converted them all to RGB images in the paper.

The first scene is an image consisting of colored sheets on a complex colored background. The scene is taken under two high frequency illuminants. Since the images under illuminants l_1 and l_2 are similar in the RGB images, we only show the scene taken under illuminant l_1 in Figure 10(a). Figure 1(b) and (c) are the corresponding recovered reflective and fluorescent components. The complex colored background sheet only has ordinary reflectance so its colors

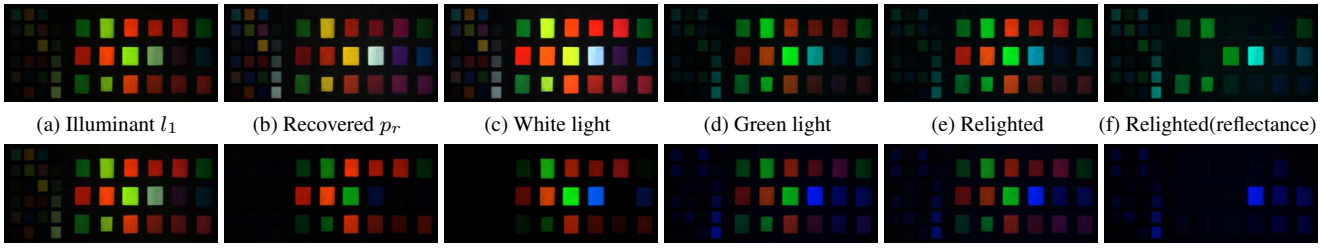

(a) Illuminant l_1 (b) Recovered p_r (c) White light (d) Green light (e) Relighted (f) Relighted(reflectance)

(g) Illuminant l_2 (h) Recovered p_f (i) Near UV light (j) Blue light (k) Relighted (l) Relighted (reflectance)

Figure 11. The separation and relighting results for color chart.

in the recovered reflective component (Figure 1(b)) is the same as those seen under white light (Figure 1(a)). Looking at the letter "C" that we cut from the pink sheet in Figure 1(a), we see that the recovered fluorescent component appears to be red. The measured emission spectrum of the pink sheet (Figure 8(e)) indicates that the color of the fluorescent component is indeed red. In addition, the scene captured under near UV light (Figure 10(b)) shows nearly pure fluorescent emission colors that also agree with our results. We note that since each fluorescent material has its own absorption spectrum, the value for $\left(\int l(\lambda^{'})a(\lambda^{'})\mathrm{d}\lambda^{'}\right)$ is different between fluorescent materials captured under near UV light and high frequency light. As a result, under different lighting, fluorescent objects can exhibit different scales of emission, but the chromaticities match well under near UV light (Figure 10(b)) and recovered fluorescent component (Figure 1(c)). Similar separation results can be found in Figures 11, 12 and 13(b) and (h).

Since our method is able to recover the full reflectance, fluorescent emission, and fluorescent absorption spectra for an entire scene, we are also able to relight scenes. Figure 10 shows that real scenes can be accurately relighted using our method. The scenes are captured under green (Figure 10(c)) and blue (Figure 10(e)) illuminants. The corresponding relighting results are shown in Figure 10(d) and (f). We can see that, the relighting results are very similar to the ground truths (Figure 10(c) and (e)), and demonstrate the effectiveness of our method to recover the reflectance and fluorescent emission and absorption spectra. When the scene is relighted using the reflective component only, (Figure 10(g) and (h)), this leads to many fluorescent materials appearing as black, especially under blue light (Figure 10(h)). Similar relighting results can be found in Figures 11, 12 and 13 (d)(e)(f)(j)(k)(l).

6. Conclusion

In this paper, we presented a method to simultaneously recover the reflectance and fluorescent emission spectra of an entire scene by using high frequency illumination in the spectral domain. Afterward, we presented, to our knowledge, the first method for estimating the fluorescent absorption spectrum of a material given its emission spectrum. Through our method, we also showed that similar emission spectra tend to map to similar absorption spectra. The effectiveness of the proposed method was successfully demonstrated with experiments using real data taken by the spectroradiometer and camera. In the future, we plan to recover the reflectance and fluorescent emission and absorption by using an RGB camera without the need for hyperspectral imaging.

References

[1] C. Balas, V. Papadakis, N. Papadakis, A. Papadakis, E. Vazgiouraki, and G. Themelis, "A novel hyper-spectral imaging apparatus for the non-destructive analysis of objects of artistic and historic value," *J. Cult. Herit.*, vol. 4, no. 1, 2003.

[2] I. B. Styles, A. Calcagni, E. Claridge, F. Orihuela-Espina, and J. M. Gibson, "Quantitative analysis of multi-spectral fundus images." *Medical Image Analysis*, vol. 10, no. 4, 2006.

[3] G. Johnson and M. Fairchild, "Full-spectral color calculations in realistic image synthesis," *IEEE Computer Graphics and Applications*, vol. 19, Aug. 1999.

[4] C. Chi, H. Yoo, and M. Ben-Ezra, "Multi-spectral imaging by optimized wide band illumination," *IJCV*, vol. 86, no. 2-3, Jan. 2010.

[5] J. M. DiCarlo, F. Xiao, and B. A. Wandell, "Illuminating illumination," in *CIC*. IS&T/SID, 2001.

[6] L. T. Maloney and B. A. Wandell, "Color constancy: a method for recovering surface spectral reflectance," *JOSA A*, vol. 3, no. 1, 1986.

[7] S. Tominaga, "Multichannel vision system for estimating surface and illumination functions," *JOSA A*, vol. 13, no. 11, Nov 1996.

[8] N. Gat, "Imaging spectroscopy using tunable filters: A review," in *Wavelet Applications VII*, vol. 4056. SPIE, 2000.

[9] J. Park, M. Lee, M. D. Grossberg, and S. K. Nayar, "Multispectral Imaging Using Multiplexed Illumination," in *ICCV*. IEEE, Oct 2007.

[10] K. Barnard, "Color constancy with fluorescent surfaces," in *IEEE Conference on Computer Vision and Pattern Recognition (CVPR)*, 1999.

[11] C. Zhang and I. Sato, "Separating reflective and fluorescent components of an image," in *IEEE Conference on Computer Vision and Pattern Recognition (CVPR)*, 2011.

[12] F. W. D. Rost, *Fluorescence Microscopy*. Cambridge University Press, 1992.

[13] D. A. Skoog, F. J. Holler, and S. R. Crouch, *Principles of Instrumental Analysis*. Thomson Publishers, 2007.

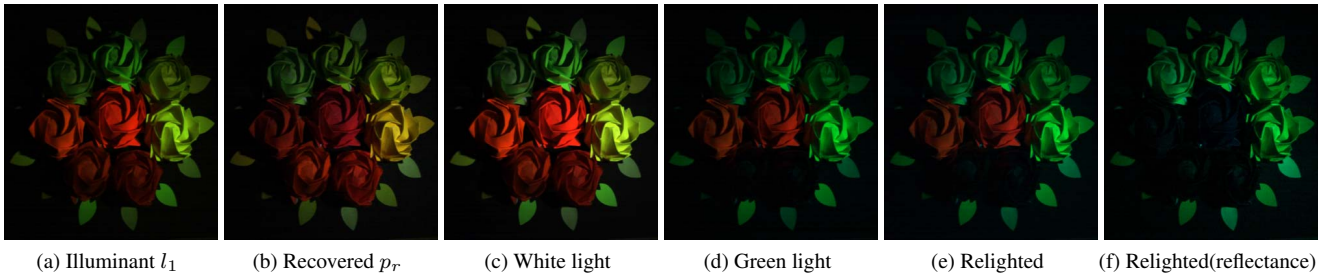

(a) Illuminant l_1 (b) Recovered p_r (c) White light (d) Green light (e) Relighted (f) Relighted(reflectance)

(g) Illuminant l_2 (h) Recovered p_f (i) Near UV light (j) Blue light (k) Relighted (l) Relighted (reflectance)

Figure 12. The separation and relighting results for a scene with fluorescent and non-fluorescent roses.

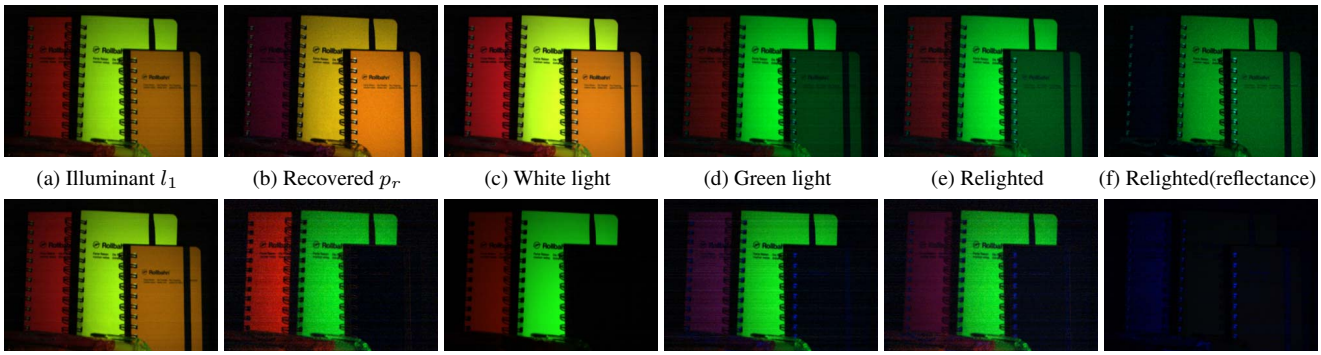

(a) Illuminant l_1 (b) Recovered p_r (c) White light (d) Green light (e) Relighted (f) Relighted(reflectance)

(g) Illuminant l_2 (h) Recovered p_f (i) Near UV light (j) Blue light (k) Relighted (l) Relighted (reflectance)

Figure 13. The separation and relighting results for a scene with fluorescent and non-fluorescent objects.

[14] S. K. Nayar, G. Krishnan, M. D. Grossberg, and R. Raskar, "Fast separation of direct and global components of a scene using high frequency illumination," *ACM Trans. Graph.*, vol. 24, no. 3, Jul. 2006.

[15] A. Springsteen, "Introduction to measurement of color of fluorescent materials," *Analytica Chimica Acta*, vol. 380, 1999.

[16] M. B. Hullin, J. Hanika, B. Ajdin, H.-P. Seidel, J. Kautz, and H. P. A. Lensch, "Acquisition and analysis of bispectral bidirectional reflectance and reradiation distribution functions," *ACM Trans. Graph.*, vol. 29, 2010.

[17] I. Sato, T. Okabe, and Y. Sato, "Bispectral photometric stereo based on fluorescence," in *Color Imaging Conference: Color Science, Systems, and Applications*, 2012.

[18] T. Treibitz, Z. Murez, B. G. Mitchell, and D. Kriegman, "Shape from fluorescence," in *European conference on Computer Vision*, 2012.

[19] M. Alterman, Y. Schechner, and A. Weiss, "Multiplexed fluorescence unmixing," in *IEEE International Conference on Computational Photography (ICCP)*, 2010.

[20] B.-K. Lee, F.-C. Shen, and C.-Y. Chen, "Spectral estimation and color appearance prediction of fluorescent materials," *Optical Engineering*, vol. 40, 2001.

[21] S. Tominaga, T. Horiuchi, and T. Kamiyama, "Spectral estimation of fluorescent objects using visible lights and an imaging device," in *Proceedinds of the IS&T/SID Color Imaging Conference*, 2011.

[22] H. Farid and E. Adelson, "Separating reflections and lighting using independent components analysis," in *Computer Vision and Pattern Recognition (CVPR)*, Fort Collins, CO, 1999.

[23] S. Nayar, X. Fang, and T. Boult, "Removal of Specularities using Color and Polarization," in *IEEE Conference on Computer Vision and Pattern Recognition (CVPR)*, Jun 1993.

[24] A. V. Oppenheim, A. S. Willsky, and w. S. Hamid, *Signals and Systems*, 2nd ed. Prentice Hall, Aug. 1996.

[25] G. McNamara, A. Gupta, J. Reynaert, T. D. Coates, and C. Boswell, "Spectral imaging microscopy web sites and data," *Cytometry. Part A: the journal of the International Society for Analytical Cytology*, vol. 69, no. 8, 2006.

[26] D. Donoho, Y. Tsaig, I. Drori, and J.-L. Starck, "Sparse solution of underdetermined systems of linear equations by stagewise orthogonal matching pursuit," *IEEE Transactions on Information Theory*, vol. 58, no. 2, 2012.

[27] E. Candes and T. Tao, "Near-optimal signal recovery from random projections: Universal encoding strategies?" *IEEE Transactions on Information Theory*, vol. 52, no. 12, 2006.

[28] B. Efron, T. Hastie, I. Johnstone, and R. Tibshirani, "Least angle regression," *Annals of Statistics*, vol. 32, 2004.